Polymer Bulletin 16, 75–82 (1986)

Polymer Bulletin

Photoconductivity of polymeric dibenz [b, i] 1, 4, 8, 11-tetraaza [14] annulenato (μ-pyrazin)iron(II) [Fetaa(pyz)]$_n$

H. Meier[1]*, W. Albrecht[1], M. Hanack[2], and J. Koch[2]

[1] Staatliches Forschungsinstitut für Geochemie, Concordiastraße 28, D-8600 Bamberg, Federal Republic of Germany

[2] Institut für Organische Chemie der Universität Tübingen, Lehrstuhl für Organische Chemie II, Auf der Morgenstelle 18, D-7400 Tübingen, Federal Republic of Germany

Dedicated to Prof. Dr. G. Manecke on the occasion of his 70th birthday

Summary: Results of experiments on dark- and photoconductivity of polymeric dibenz[b,i]1,4,8,11-tetraaza[14]annulenato-(μ-pyrazin)iron(II) [Fetaa(pyz)]$_n$ are described. By studying the dependence of photoconductivity on electric field, intensity and wavelength it is shown that photogeneration of charge carriers occurred at short wavelengths by an Onsager mechanism and in the near-infrared region by a photoinjection process from the electrodes.

1. Introduction

It has recently been demonstrated that polymeric phthalocyanines formed by polymerization of squareplanar phthalocyanine rings to linear chains exhibit photoelectric properties (MEIER et al. 1985a, 1985b). For instance, polymeric μ-cyano-phthalocyaninato-cobalt(III) which is characterized by a high dark conductivity (DATZ et al. 1984, METZ and HANACK 1985) can be considered as an organic photoconductor with a remarkable photoelectric sensitivity (MEIER et al. 1985b). This observation suggests that for applications, e.g. as components in photovoltaic devices, organic photoconductors with relatively high thermal conductivity and appreciable stability in air may become available.

However, no experimental results are known to us showing correlations of different combinations of macrocycles(X_4), bridging ligands(L) and central metal atoms(M) to the photoelectric properties of this type of one-dimensional conductor [X_4ML]$_n$. Therefore, studies seem necessary for completing data on the effect of chemical structure by including polymers with different bridged structures and metals.

In this paper first results of studies on dark- and photoconductivity of polymeric dibenz[b,i]1,4,8,11-tetraaza[14]annulenato(μ-pyrazin)iron(II) are given.

2. Experimental

Polymeric dibenz[b,i]1,4,8,11-tetraaza[14]annulenato(μ-pyrazin)iron(II), abbreviated as [Fetaa(pyz)]$_n$, has been synthe-

* To whom offprint requests should be sent

sized as described by KOCH and HANACK (1983).

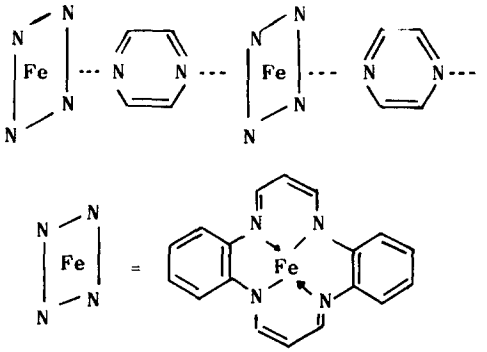

The photoelectric properties of $[Fetaa(pyz)]_n$ have been measured without any additive in surface-type cells employing copper/zinc contacts with electrode distances of 0.2 mm (MEIER et al. 1982). In addition, dark conductivity was investigated in sandwich-type cells of compressed pellets (thickness L $\approx$ 1.6 mm).

The samples were measured at pressures of 10^{-5} - 10^{-6} Torr and 1 bar, respectively, in the temperature range of 298 - 395 K. Dark- and photocurrents were registered with a Keithley 480 picoammeter in combination with a fast recorder.

The light source consisted of a 1000 W xenon lamp, focussed by quartz lenses on to the photoelectric cell. Monochromatic light in the spectral range 350 - 1900 nm was obtained with band pass filters with band widths of 50 nm (Schott). Light intensities were varied with neutral density filters and recorded with a Moll thermopile.

3. Results and discussion

3.1. Dark conductivity

The variation of dark conductivity σ_D with temperature can be described by

$$\sigma_D = \sigma_o \exp(-\Delta E/2kT) \qquad (1)$$

where k = Boltzmann's constant, T = absolute temperature, σ_o = pre-exponential conductivity and ΔE = activation energy. The parameters derived from an Arrhenius plot given in Fig. 1 are ΔE = 0.93 eV and $\sigma_o = 5.8 \times 10^2 \Omega^{-1}$ cm^{-1} at T $>$ 290 K.

The increase of dark conductivity with temperature corresponding to Eq. (1) is typical for organic semiconductors (GUTMAN and LYONS 1967, MEIER 1974). It may result from a direct generation of carriers across an energy gap or by an excitation of donor or acceptor states.

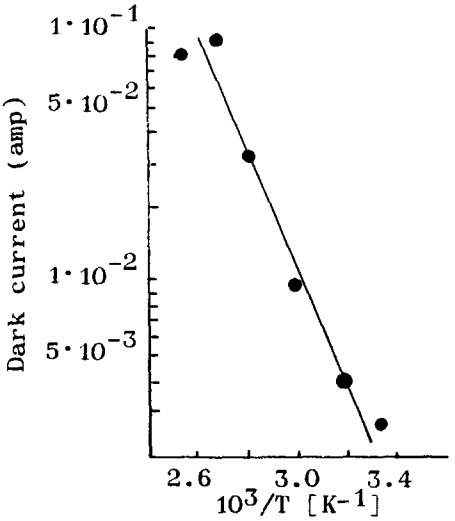

Fig. 1 Temperature dependence of dark current of $[Fetaa(pyz)]_n$. U = 100 V. L = 1.6 mm.

In this context, it is remarkable that dark currents increase with increasing voltage according to

$$I_D = aU^s \qquad (2)$$

where U is voltage and a is a constant with $s \simeq 1$. The parameter $s \simeq 1$ points at ohmic conductivity due to thermally generated carriers. Therefore, injection of carriers from the electrodes does not seem to be dominant.

3.2. Photoconductivity

As in polymeric phthalocyanines, such as $[PcGeS]_x$ and $[PcCoCN]_x$, the conductivity of $[Fetaa(pyz)]_n$ increases rapidly (i.e., within 1 s) on irradiation with visible light. In discussing the photoresponse of $[Fetaa(pyz)]_n$ the following relationships should be taken into account:

1. Photocurrents increase with light intensity I_B, yielding curves of

$$I_{ph} = bI_B^{\gamma} \qquad (3)$$

as shown in Fig. 2 (b = constant. γ = intensity parameter).

The parameter $\gamma = 0.89$ (T = 298 K) can be understood if we assume photosensitive ohmic currents in the presence of exponentially distributed traps that control currier recombination (ROSE 1963, MEIER 1974). In this case the photocurrent will be approximately given by

$$I_{ph} \sim I_B^{T_c/T_c+T} \quad (4)$$

resulting in T_c of the order of 2400 K. This high T_c value points to exponentially distributed traps that may behave approximately like linear distributed trapping states.

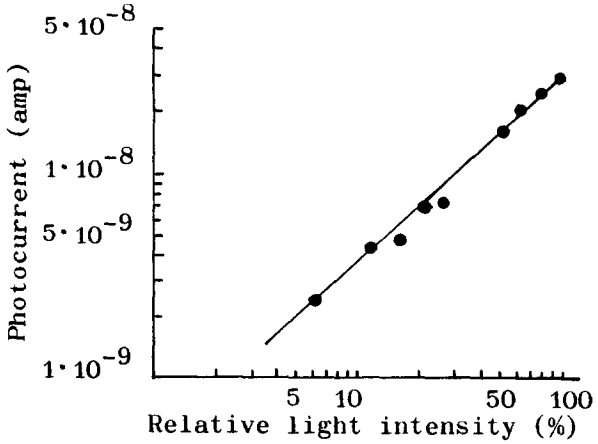

Fig. 2 Dependence of photocurrent on light intensity in $[Fetaa(pyz)]_n$. λ = 647 nm. U = 70 V. I_B (100 %) = 5.4 x 10^{15} photons s^{-1} per sample surface.

2. Photocurrents increase with increasing voltage corresponding to

$$I_{ph} = \bar{a}U^{\bar{s}} \quad (5)$$

as demonstrated in Fig. 3 ($\bar{a}$ = constant. $\bar{s}$ = voltage parameter).

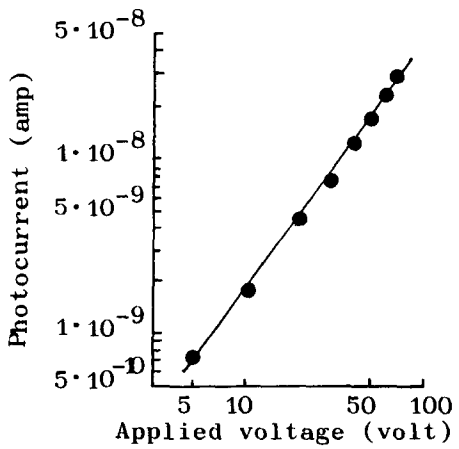

Fig. 3 Dependence of photocurrent on applied voltage in $[Fetaa(pyz)]_n$. I_B (unfiltered) ≈ 20 mW per sample.

The parameter $\bar{s}$ = 1.4 is in agreement with the ohmic character of the photocurrent.

3. The photoconductive spectrum of $[Fetaa(pyz)]_n$ is characterized by a main peak at 350 nm and a small peak at about 420 nm followed by a broad photoconductive band in the long-wavelength part of the spectrum (see Fig. 4). In Fig. 4 as measure of the relative photoconductivity the parameter $I_{ph}^{1/\gamma}/Nq$ is given because of its independence of the incident photon flux Nq.

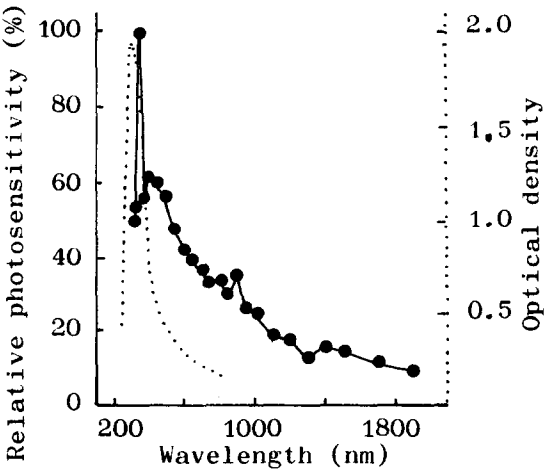

Fig. 4 Photoconductive spectrum of $[Fetaa(pyz)]_n$ (plotted as $I_{ph}^{1/\gamma}/Nq$ in rel.%) and absorption spectrum in KBr (dotted line).

For comparing photosensitivity of $[Fetaa(pyz)]_n$ in the short-wavelength region and in the long-wavelength part of the spectrum the following points should be noted:

(a) The action spectrum of $[Fetaa(pyz)]_n$ corresponds largely with the absorption spectrum. There is only a small shift of about 60 nm of the photoresponse to longer wavelengths. Therefore, one can discuss an intrinsic photogeneration process. Because a plot of I_{ph}/E versus E gives in accordance with Eq. (6)

$$I_{ph}/E = (e\mu\tau I_A V/L)\eta_o \exp(-r_c/r_o)\ (1 + er_cE/2kT) \qquad (6)$$

a linear dependence as shown in Fig. 5 the generation of free carriers may be caused by the Onsager two-step mechanism (ONSAGER 1938, BATT et al. 1969). In Eq. 6 e = electronic charge, μ = mobility, τ = carrier lifetime, I_A = number of photons per s and cm^3, V = volume of the sample, L = electrode distance, η_o = primary quantum yield, r_o = initial charge separation distance, r_c = Onsager distance, E = field strength.

From least-squares analysis of this plot a slope to intercept ratio of 6.7 x 10^{-4} cm/V is obtained. This value exceeds the value predicted by the Onsager model which (corresponding to $er_c/2kT$) is 3.4 x 10^{-5} cm/V at 296 K (with ϵ = 3.2). However,

the difference between experimental and theoretical values may be attributed to free carrier-trapped carrier recombination (CHANCE and BRAUN 1973).

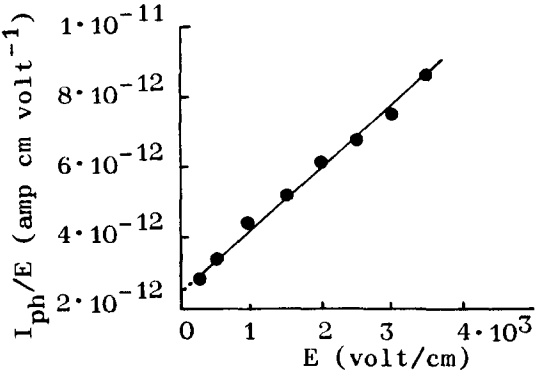

Fig. 5 Plot of I_{ph}/E vs. electric field E for $[Fetaa(pyz)]_n$. λ = 647 nm. T = 296 K.

(b) The long-wavelength photoresponse may be explained by photo-injection of charge carriers into $[Fetaa(pyz)]_n$ from electrodes like in anthracene single crystals and polycrystalline 2,4,7-trinitro-9-fluorenone films (BAESSLER and KILLESREITER 1972, BULYSHEV et al. 1984). In agreement with this mechanism a Fowler plot (see FOWLER 1931) of the quantum efficiency $\bar{G}^{1/2}$ versus $h\nu$ (eV) gives according to

$$\bar{G} \sim (h\nu - \varphi)^2 \qquad (7)$$

a linear dependence as demonstrated in Fig. 6 (φ = threshold energy). From extrapolating of this plot a threshold energy φ = 0.32 eV for photoinjection of charge carriers into $[Fetaa(pyz)]_n$ is obtained.

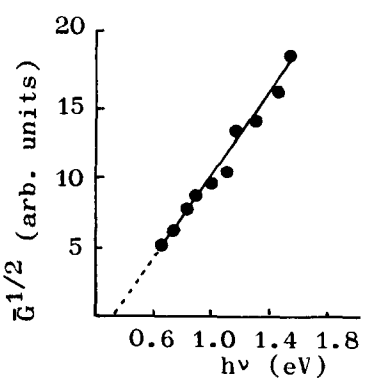

Fig. 6 Fowler plot for $[Fetaa(pyz)]_n$ at E = 2.5 x 10^2 V/cm.

4. An estimate of the photoconductive gain G, defined as the number of charge carriers passing through the sample per absorbed photon, according to Eq. 8

$$G = \frac{I_{ph}/e}{I_A V} \qquad (8)$$

gives $G \simeq 5.9 \times 10^{-5}$ at $\lambda = 355$ nm and $E = 2.5 \times 10^3$ V/cm. From plots of the product of gain and electrode distance against the field the mean distance of the carrier drift ($\mu\tau E$, Schubweg; $\mu\tau$, carrier range) can be derived because we have the relation

$$\log (GL) = \log (\eta\mu\tau) + z \log E \qquad (9)$$

(z = constant). These parameters are necessary for describing photovoltaic characteristics under solar light (GALLUZZI 1985). The values are $\mu\tau = 6.7 \times 10^{-12}$ cm^2, $\mu\tau E = 1.3 \times 10^{-8}$ ($E = 2 \times 10^3$ V/cm) if the carrier generation efficiency would have the value $\eta \simeq 1$ (see Fig. 7).

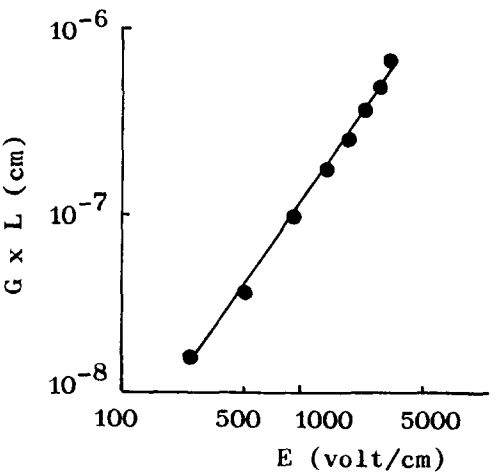

Fig. 7 Plot of G·L against the field for $[Fetaa(pyz)]_n$ at 647 nm.

4. Conclusion and Acknowledgement

It can be stated that $[Fetaa(pyz)]_n$ shows photocurrents that depend on intensity, voltage and wavelength. Contrary to $[PcGeS]_x$ and $[PcCoCN]_x$ photoconductivity action spectra are characterized by definite peaks in the short-wavelength region ($\lambda < 450$ nm) and by a broad photoconductivity band in the long-wavelength part of the spectrum ($\lambda > 700$ nm). Photoconducti-

vity in the short-wavelength region probably can be explained by an Onsager mechanism and at longer wavelength by photoinjection of charge carriers from electrodes.

The authors would like to thank the Volkswagen Foundation for financial support.

5. Literature references

BATT, R.H., BRAUN, C.L. and HORNIG, J.F.: Appl. Optics, Suppl. 3: Electrophotography (1969) pp. 20

BAESSLER, H. and KILLESREITER, H.: Phys. stat. sol. (b) 53, 183 (1972)

BULYSHEV, Yu.S., KASHIRSKII, I.M. and SINITSKII, V.V.: Phys. stat. sol. (a) 82, 537 (1984)

CHANCE, R.R. and BRAUN, C.L.: J. Chem. Phys. 59, 2269 (1973)

DATZ, A., METZ, J., SCHNEIDER, O. and HANACK, M.: Synth. Met. 9, 31 (1984)

FOWLER, R.H.: Phys. Rev. 38, 45 (1931)

GALLUZZI, F.: J. Phys. D.: Appl. Phys. 18, 685 (1985)

GUTMAN, F. and LYONS, L.E.: Organic Semiconductors, Wiley, New York 1967

KOCH, J. and HANACK, M.: Chem. Ber. 116, 2109 (1983)

METZ, J. and HANACK, M.: J. Am. Chem. Soc. 105, 828 (1985)

MEIER, H.: Organic Semiconductors: Dark- and Photoconductivity of Organic Solids, Verlag Chemie, Weinheim 1974

MEIER, H., ALBRECHT, W. and ZIMMERHACKL, E.: Report I/60075, Volkswagen Foundation, Hannover, 1982, pp. 5

MEIER, H., ALBRECHT, W., ZIMMERHACKL, E., HANACK, M. and FISCHER, K.: J. Mol. Electronics 1, 47 (1985a)

MEIER, H., ALBRECHT, W., ZIMMERHACKL, E., HANACK, M. and METZ, J.: Synth. Met. 11, 333 (1985b)

ONSAGER, L.: Phys. Rev. 54, 554 (1938).

Accepted July 2, 1986